Reduction of stratum corneum ceramides in Neu-Laxova syndrome caused by phosphoglycerate dehydrogenase deficiency[S]

Takuya Takeichi,[1,*] Yusuke Okuno,[†,§] Akane Kawamoto,[**] Takeshi Inoue,[††] Eiko Nagamoto,[§§] Chiaki Murase,[*] Eri Shimizu,[***] Kenichi Tanaka,[††] Yuichi Kageshita,[§§] Satoshi Fukushima,[§§] Michihiro Kono,[*] Junko Ishikawa,[**] Hironobu Ihn,[§§] Yoshiyuki Takahashi,[§] and Masashi Akiyama[1,*]

Department of Dermatology* and Department of Pediatrics,[§] Nagoya University Graduate School of Medicine, Nagoya 466-8550, Japan; Center for Advanced Medicine and Clinical Research,[†] Nagoya University Hospital, Nagoya 466-8550, Japan; Biological Science Research Laboratories** and Analytical Science Research Laboratories,*** Kao Corporation, Haga, Tochigi 321-3497, Japan; and Department of Pediatrics[††] and Department of Dermatology and Plastic Surgery,[§§] Faculty of Life Sciences, Kumamoto University, Kumamoto 860-8556, Japan

Abstract Neu-Laxova syndrome (NLS) is a very rare autosomal recessive congenital disorder characterized by disturbed development of the central nervous system and the skin and caused by mutations in any of the three genes involved in de novo L-serine biosynthesis: *PHGDH*, *PSAT1*, and *PSPH*. L-Serine is essential for the biosynthesis of phosphatidylserine and sphingolipids. The extracellular lipid of the stratum corneum, of which sphingolipid constitutes a significant part, plays a primary role in skin barrier function. Here, we describe a Japanese NLS pedigree with a previously unreported nonsense mutation in *PHGDH* and a unique inversion of chromosome 1. In addition, the levels of 11 major ceramide classes in the tape-stripped stratum corneum of the NLS patient's skin were assessed by LC/MS. Notably, lower amounts of ceramides of all classes were found in the patient's stratum corneum than in those of controls. This is the first report to demonstrate the reduction of ceramides in the stratum corneum of an NLS patient due to *PHGDH* mutations. The clinical findings and a detailed analysis of ceramides from the stratum corneum in the family extend the spectrum of clinical anomalies and give us a clue to the pathomechanisms of ichthyosis in NLS patients with phosphoglycerate dehydrogenase deficiency.—Takeichi, T., Y. Okuno, A. Kawamoto, T. Inoue, E. Nagamoto, C. Murase, E. Shimizu, K. Tanaka, Y. Kageshita, S. Fukushima, M. Kono, J. Ishikawa, H. Ihn, Y. Takahashi, and M. Akiyama. **Reduction of stratum corneum ceramides in Neu-Laxova syndrome caused by phosphoglycerate dehydrogenase deficiency. *J. Lipid Res.* 2018.** 59: **2413–2420.**

Supplementary key words ceramide • skin barrier • ichthyosis • L-serine • sphingolipid

Neu-Laxova syndrome (NLS) is a term that unifies the independent reports by Neu and Laxova of a lethal multiple congenital anomaly syndrome (1). The main features of NLS involve defective somatic growth and the disturbed development of the central nervous system and skin, as well as many other anomalies that might present primarily as malformations or a malformation sequence (1). In 2014, mutations in *PHGDH*, which encodes phosphoglycerate dehydrogenase (PHGDH), were found in autosomal recessive cases of NLS (1). In addition, mutations in *PSAT1*, which encodes phosphoserine aminotransferase 1, and *PSPH*, which encodes phosphoserine phosphatase, were identified in several autosomal recessive cases of NLS (2). NLS is a genetically heterogeneous disorder that can be caused by mutations in any of the three genes involved in de novo L-serine biosynthesis: *PHGDH*, *PSAT1*, and *PSPH* (**Fig. 1**). L-Serine is a nonessential amino acid that is synthesized de novo from the glycolytic intermediate 3-phosphoglycerate through three steps that are respectively catalyzed by PHGDH, phosphoserine aminotransferase, and phosphoserine phosphatase (3).

PHGDH deficiency, which is a congenital error of serine metabolism, was first described in 1996, before NLS was proposed as a syndrome (4). PHGDH is the first enzyme in the de novo biosynthesis of serine from carbohydrates. A reduced ability to synthesize L-serine has potentially serious consequences for cellular metabolism (5). Serine is

This work was supported by Japan Agency for Medical Research and Development Grant JP18gm0910002 (M.A.) and Japan Society for the Promotion of Science Grants-In-Aid 18H02832 (M.A.) and 18K16058 (T.T.) for Scientific Research (B) and Young Scientists, respectively. The authors declare that there are no conflicts of interest.

Manuscript received 6 June 2018 and in revised form 21 October 2018.

Published, JLR Papers in Press, October 22, 2018
DOI https://doi.org/10.1194/jlr.P087536

This article is available online at http://www.jlr.org

Abbreviations: deoxySL, 1-deoxysphingolipid; HSAN1, hereditary sensory and autonomic neuropathy type 1; NLS, Neu-Laxova syndrome; PHGDH, phosphoglycerate dehydrogenase; WES, whole-exome sequencing; WGS, whole-genome sequencing.

[1] To whom correspondence should be addressed.
e-mail: takeichi@med.nagoya-u.ac.jp (T.T.);
makiyama@med.nagoya-u.ac.jp (M.A.)

[S] The online version of this article (available at http://www.jlr.org) contains a supplement.

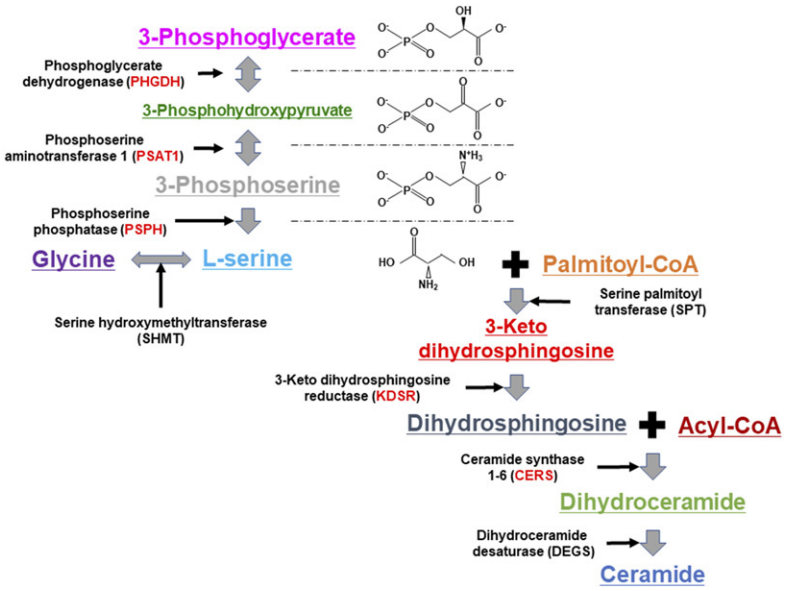

Fig. 1. Simple schema of L-serine biosynthesis pathway and de novo synthetic pathway of ceramides. Pathways, key enzymes, and the chemical structures of the substrates/products in the first three enzymes steps. The red enzymes are known to be causative molecules for congenital ichthyosis.

incorporated directly into proteins and is a precursor for the de novo biosynthesis of glycine, cysteine, and the nonstandard amino acid selenocysteine. It is also essential for the biosynthesis of phosphatidylserine and sphingolipids (5). The extracellular lipid of the stratum corneum, of which sphingolipid constitutes a significant part, plays a primary role in skin barrier function (6). Because serine is a precursor of sphingolipids, it is possible that defective sphingolipid synthesis due to serine deficiency affects the stratum corneum (3). There are more than 1,000 ceramide species, most of which are present in the cutaneous stratum corneum (7). The major route of ceramide formation is the salvage pathway, which delivers 50% to 90% of the ceramide and uses the hydrolysis of sphingomyelin by sphingomyelinase (8). Ceramide can also be synthesized de novo in the endoplasmic reticulum (8). The first step in the de novo pathway of ceramide synthesis is catalyzed by serine palmitoyl transferase, condensing L-serine and palmitoyl-CoA to generate 3-ketodihydrosphingosine (Fig. 1) (9).

To date, 19 pathogenic mutations in *PHGDH* have been reported in PHGDH deficiency and NLS (www.hgmd.cf.ac.uk) (3). Here, we describe a Japanese NLS pedigree with a nonsense mutation in *PHGDH* and an inversion of chromosome (chr) 1. Moreover, autopsy findings and a detailed ceramide analysis from the stratum corneum in the family extend the spectrum of clinical anomalies and stratum corneum lipid abnormalities resulting from PHGDH deficiency.

MATERIALS AND METHODS

Whole-exome sequencing

Exome capture was performed by in-solution hybridization using SureSelect Human All Exon V5 bait (Agilent Technologies, Santa Clara, CA). Massively parallel sequencing was performed with the Illumina HiSeq2500 platform with 150 bp paired-end reads (Illumina, San Diego, CA). The reads produced were aligned to the hg19 reference human genome using the Burrows-Wheeler Aligner software with default parameters and a -mem option (10). PCR duplicates were removed using MarkDuplicates in Picard tools (https://broadinstitute.github.io/picard). Candidate variants were called using VarScan 2 (http://massgenomics.org/varscan) and annotated using ANNOVAR (http://annovar.openbioinformatics.org). Common variants defined by >1% minor allele frequency in ExAC (http://exac.broadinstitute.org), 1000 Genomes (http://www.1000genomes.org), or ESP6500 (http://evs.gs.washington.edu/EVS) were excluded from analysis.

Whole-genome sequencing

Whole-genome sequencing (WGS) was performed using the HiSeq X platform (Illumina). Alignment and variant calling were performed in the same way as in whole-exome sequencing (WES). The detection of structural variations was performed with our in-house software. Briefly, soft-clipped bases on reads with a mapping quality >30 were realigned to the human genome using BLAT with default parameters and stepSize = 5. A candidate was judged to be a structural variation if there were three or more supporting reads and was further inspected by Integrative Genomics Viewer (11).

Immunohistochemical analyses

Immunohistochemical analysis of skin samples from the participants was performed as described previously (12) with slight modifications. Thin sections (3 μm) were cut from samples embedded in paraffin blocks. The sections were soaked for 20 min at room temperature in 0.3% H_2O_2-methanol to block endogenous peroxidase activity. After washing in PBS with 0.01% Triton X-100, the sections were incubated for 30 min in PBS with 4% BSA followed by an overnight incubation with the primary antibody, monoclonal mouse anti-PHGDH antibody (ab57030; Abcam, Cambridge, UK), in PBS containing 1% BSA. After washing in PBS, the thin sections were stained with avidin-conjugated goat anti-mouse immunoglobulin secondary antibodies for 1 h at room temperature and washed in PBS. The Vectastain Elite ABC-PO kit (Vector Laboratories, Burlingame, CA) was used for staining.

Tape stripping and lipid analysis by LC/MS

To examine the ceramide species present in the stratum corneum, tape stripping was performed by pressing and stripping an adhesive acrylic film (465#40; Teraoka Seisakusho, Tokyo, Japan) from the skin of the right leg of Case 2. Samples were also taken

from the right leg of 12 normal neonates (4–5 weeks after birth) as controls. Five consecutive tape strips (15 × 50 mm) were obtained from a single individual. The samples were then subjected to LC/MS analysis to assess the levels of 11 major ceramide species (13, 14). The tape strips were cut into two half-strips: one for lipid analysis and the other for protein analysis. The lipids within the first half-strip were dissolved in 2 ml chloroform-methanol-2-propanol (10:45:45; v/v/v). *N*-Heptadecanoyl-D-erythro-sphingosine (d18:1/17:0) (Avanti Polar Lipids, Alabaster, AL) was added as an internal control, and its final concentration was 50 nmol/l. This lipid solution was subjected to reverse-phase LC/MS. The system was an Agilent 6130 Series LC/MSD system equipped with a multi-ion source, ChemStation software, an Agilent 1260 Infinity Series LC, and an L-column octadecylsilyl (2.1 mm internal diameter × 150 mm; Chemicals Evaluation and Research Institute). Chromatographic separation of the lipids was achieved at a flow rate of 0.2 ml/min using a mobile-phase binary gradient solvent system. Each ceramide species was detected by selected ion monitoring of *m/z* $[M+CH3COO]^-$. Soluble proteins were extracted from the other half-strip with 0.1 mol/l NaOH of 1% sodium dodecyl sulfate aqueous solution at 60°C for 150 min. The extract solutions were then neutralized with an HCl aqueous solution. Soluble proteins were then measured using a BCA protein assay kit (Thermo Fisher Scientific, Waltham, MA).

Analysis of free amino acids in the stratum corneum

Five consecutive tape strips (20 × 25 mm) were taken from the skin by pressing and stripping an adhesive acrylic film (465#40; Teraoka Seisakusho) from the skin of the right leg of Case 2. The tapes were immersed in 2 ml methanol-water (9:1; v/v) and sonicated. The extracts were dried in a nitrogen stream and were then dissolved in 0.2 ml ultrapure water. Each sample solution was placed in an ion-exchange column (#2622SC; Hitachi, Tokyo, Japan) and a Hitachi L-8800 amino acid analyzer to measure 17 free amino acids: Asp, Thr, Ser, Glu, Pro, Gly, Ala, Cys, Val, Met, Ile, Leu, Tyr, Phe, Lys, His, and Arg (15, 16). A standard amino acid solution (Wako, Osaka, Japan) was used to generate a calibration curve.

RESULTS

Cases

Case 1 was the first child born to nonrelated parents without any family history of similar disorders. His mother became pregnant from artificial insemination because of undetectable infertility. At 21 weeks of gestational age, fetal growth retardation was noticed. Prenatal magnetic resonance imaging of the fetus at 31 weeks of gestational age confirmed encephalopathy. At 32 weeks of gestational age, he was delivered by caesarean section with a birth weight of 953 g. He was admitted to the neonatal intensive care unit to receive appropriate therapy for respiratory failure.

On examination, he showed a collodion membrane on his entire body surface with deep fissuring at the joints (**Fig. 2A**). He had microcephaly with convulsions and

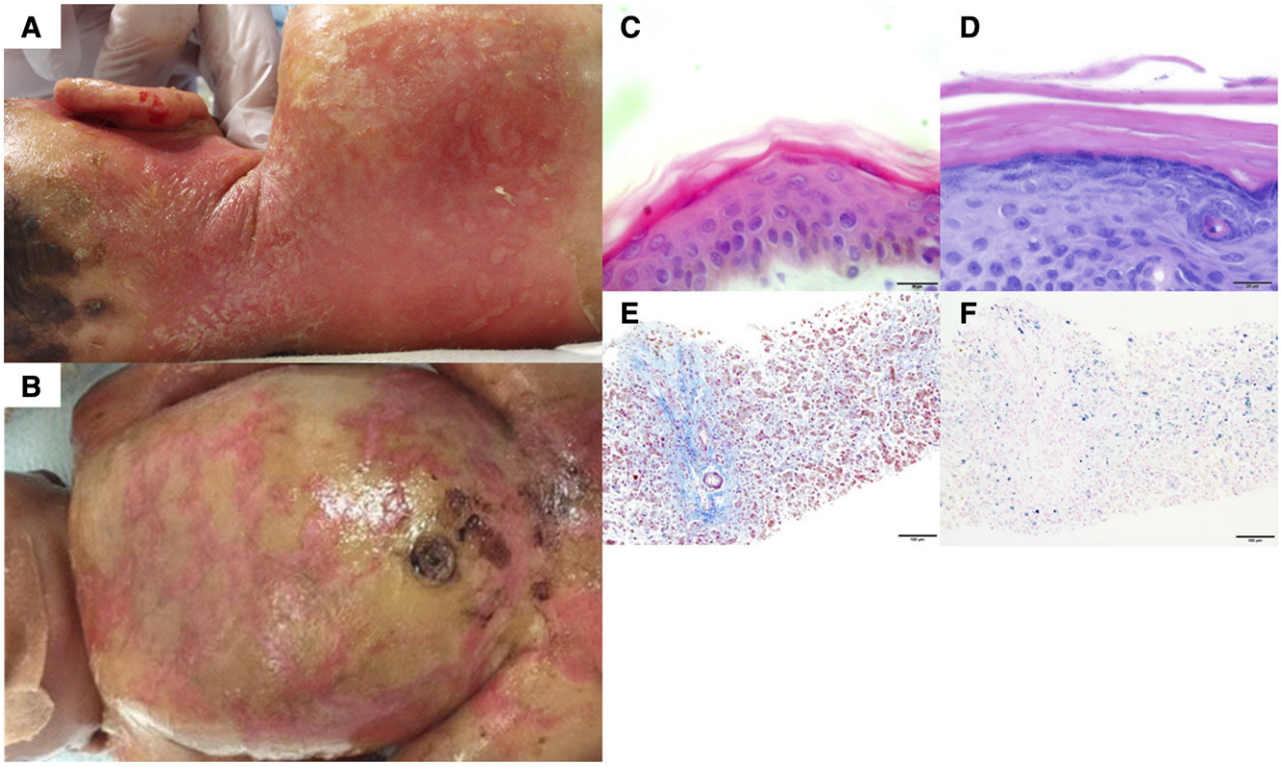

Fig. 2. Clinical and histological features of the patients. A: Case 1. Diffuse erythematous lesions with fine whitish scales are seen on the back and neck. Alopecia on the scalp and an erosion on the right ear are also observed. B: Case 2. Collodion membrane-like hyperkeratosis is seen on the chest and abdomen. C, D: A biopsy sample from the ichthyotic skin of Case 1 (D) shows compact hyperkeratosis, which suggests deficiency of the intercellular lipid layers in the stratum corneum; in contrast, the stratum corneum of the normal control skin shows a basket-weave pattern (C). The basket-weave pattern is formed by the extraction of the abundant intercellular lipids during the process of paraffin embedding the skin samples. Scale bars = 20 µm. E, F: Tissue sections of the liver from the deceased patient (Case 1) were stained with Azan stain (E) and Berlin blue (F). Severe fibrosis (E) and hemosiderin deposition (F) are observed in the liver. Scale bars = 100 µm.

several facial abnormalities (hypertelorism, flattened nose, and low auricles). He also showed moderate pancytopenia (**Table 1**) and received frequent blood transfusions and the injection of granulocyte colony-stimulating factor. A skin biopsy specimen showed compact hyperkeratosis with a normal-appearing granular layer (Fig. 2D). He had recurrent infections and was treated with several systemic antibiotics. The neutrophil phagocytic/sterilizing functions and phytohemagglutinin-induced lymphocyte blast transformation test were normal. Elevated serum liver enzymes and direct bilirubin and hepatomegaly were seen from 2 months of age (Table 1). At the age of 3 months, widespread superficial dermatophytosis was noted. Retinopathy of prematurity and cataracts were observed. The level of glucocerebrosidase was normal. Despite intensive care in the neonatal intensive care unit, he died at the age of 5 months and 21 days.

Case 2, the younger sister of Case 1, was delivered by caesarean section at 38 weeks of gestational age with a birth weight of 1,358 g. Apgar scores were 1 and 2 at 1 and 5 min, respectively. On examination, she also was found to have a collodion membrane and skin fragility (Fig. 2B). She received ventilator management for severe neonatal asphyxia. She died at the age of 5 weeks and 6 days from severe pulmonary infection.

Mutation detection

To identify the underlying molecular genetic defects in Cases 1 and 2, we obtained blood, saliva, and skin samples from the patients and blood samples from their parents for genetic testing in accordance with the Declaration of Helsinki. Results of the initial chromosomal test using genomic DNA extracted from peripheral blood from Case 1 were unremarkable. WES was then performed for Case 1 and his parents (**Table 2**). While examining the filtered rare variant list generated from the whole-exome data, we identified a rare heterozygous nonsense mutation (c.1518G>A, p.Trp506*: rs779159301) in *PHGDH*. The global allele frequency of rs779159301 is 4.069e-6. [Only one heterozygous carrier in European (non-Finnish) ethnicities has been reported in the gnomAD database (http://gnomad.broadinstitute.org), which includes 123,136 whole-exome and 15,496 whole-genome data.) Sanger sequencing confirmed that Case 1 and his father were heterozygous for this mutation (**Fig. 3A**), but no second mutation was found in the exome data of the patient or that of his mother. In addition, the whole-exome data showed no putative mutations in *PSAT1* or *PSPH* or in any other genes previously implicated in the molecular pathology of ichthyosis.

Next, we investigated whether there was an abnormality in RNA by RT-PCR using RNA extracted from the skin of Case 1. Notably, sequencing of cDNA in exon 12 of *PHGDH* demonstrated a homozygous or hemizygous condition of the paternal mutation (Fig. 3A), suggesting that there were some problems in the other allele of Case 1 (e.g., exon skipping or other transcriptional abnormalities). We then performed WGS analysis using genomic DNA from the proband's mother, because there was not enough DNA of the deceased proband (Case 1). As a result, WGS identified an approximately 1.2 Mb intragenic inversion on chr 1 (Fig. 3C). The inversion spans 1.2 Mb of genomic DNA (the accurate inversion points in intron 1 of *PHGDH* and the centromere of chr 1, chr1:120,260,529-121,484,680; GRCh37/hg19), and at the protein level it removes part of the first substrate binding domain and all of the NAD/NADP binding domain, the second substrate binding domain, and the regulatory domain of PHGDH (eliminating 487 amino acids at the C terminus of the PHGDH polypeptide) (Fig. 3C) (17). Sanger sequencing for this inversion region using a specifically designed primer pair revealed this inversion of chr 1 to be seen not only in the DNA of the mother but also in that of Case 1 (Fig. 3B). In addition, Sanger sequencing revealed Case 2 to be a compound heterozygous carrier of these two mutations (Fig. 3D). Accordingly, we diagnosed both siblings as having NLS caused by biallelic genetic defects associated with *PHGDH*.

TABLE 1. Results of blood analysis in Case 1

	At Birth	Three Months	Five Months	Normal Range
WBC count	3.2	N/A	2.4	$3.3–8.6 \times 10^3$ μL
Neutrophil count	N/A	N/A	1.3	$1.8–7.6 \times 10^3$ μL
Lymphocyte count	N/A	N/A	0.8	$0.7–3.8 \times 10^3$ μL
Hemoglobin	14.1	N/A	9.5	13.7–16.8 g/dl
Thrombocyte count	11.7	N/A	2.5	$15.8–34.8 \times 10^4$ μL
Total protein	4.8	4.5	N/A	6.6–8.1 g/dl
Albumin	3.4	2.8	1.8	4.1–5.1 g/dl
AST	18	565	318	13–30 U/L
ALT	9	339	162	10–42 U/L
Total bilirubin	1.9	9.1	14.6	0.4–1.5 mg/dl
Direct bilirubin	N/A	6.7	11.7	0–0.2 mg/dl
g-GTP	N/A	322	66	13–64 U/L
BUN	6.2	8.0	7.0	8–20 mg/dl
Creatinine	0.47	0.06	0.06	0.65–1.07 mg/dl
Calcium	9.6	9.4	8.7	8.8–10.1 mg/dl
C-reactive protein	0	1.5	10.49	<0.14 mg/dl
IgG	666	N/A	N/A	1,000–1,800 mg/dl
IgM	6	N/A	N/A	65–260 mg/dl
Procalcitonin	N/A	0.40	0.87	<0.5 ng/ml

ALT, alanine aminotransferase; AST, aspartate aminotransferase; BUN, blood urea nitrogen; N/A, not analyzed; WBC, white blood cell.

TABLE 2. Coverage data of WES

Sample	Total Reads	Mean Coverage	2× Coverage	10× Coverage	20× Coverage
Case 1	63,792,380	119.15029	0.897472	0.771792	0.704864
Father	63,522,002	100.026302	0.991876	0.982871	0.962341
Mother	58,303,690	95.947136	0.98631	0.95883	0.920685

Autopsy findings of Case 1

A partial autopsy was carried out with the informed consent of the parents. The liver architecture was severely disrupted by fibrosis (Fig. 2E), intrahepatic cholestasis, and hemosiderin deposition (Fig. 2F). There were no significant abnormalities or inflammation in the intrahepatic bile duct. Severe blood congestion and hemosiderin deposition were seen in the spleen. The bone marrow was dry tap with reduced megakaryocytes, hyper phagocytoses, and hemosiderin deposition.

Immunohistochemical analysis of the skin specimen from Case 1

We conducted an immunohistochemical analysis with an anti-PHGDH antibody in a lesional skin sample from Case 1 to assess whether the expression of PHGDH was altered at the protein level. There was significantly less immunoreactivity for PHGDH in the skin of Case 1 than in control skin (Fig. 3E, F).

Ceramide and free amino acid profile in the stratum corneum of Case 2

The levels of 11 major ceramide classes in the tape-stripped skin samples from the right leg of Case 2 were assessed by LC/MS. The level of total ceramide was significantly lower in Case 2 than in the normal controls [**Fig. 4A**; approximately 8.5% of that in the normal controls (mean − 2.6 SDs)]. Notably, all ceramide classes were significantly reduced in the Case 2 samples (Fig. 4B). Next, we investigated whether short-chain (or long-chain) ceramides increased in each ceramide class of the Case 2 samples. The average carbon numbers of ceramides indicated that CER[NDS], CER[NS], CER[NH], CER[NP], CER[ADS], CER[AS], and CER[AH] were decreased relative to those of

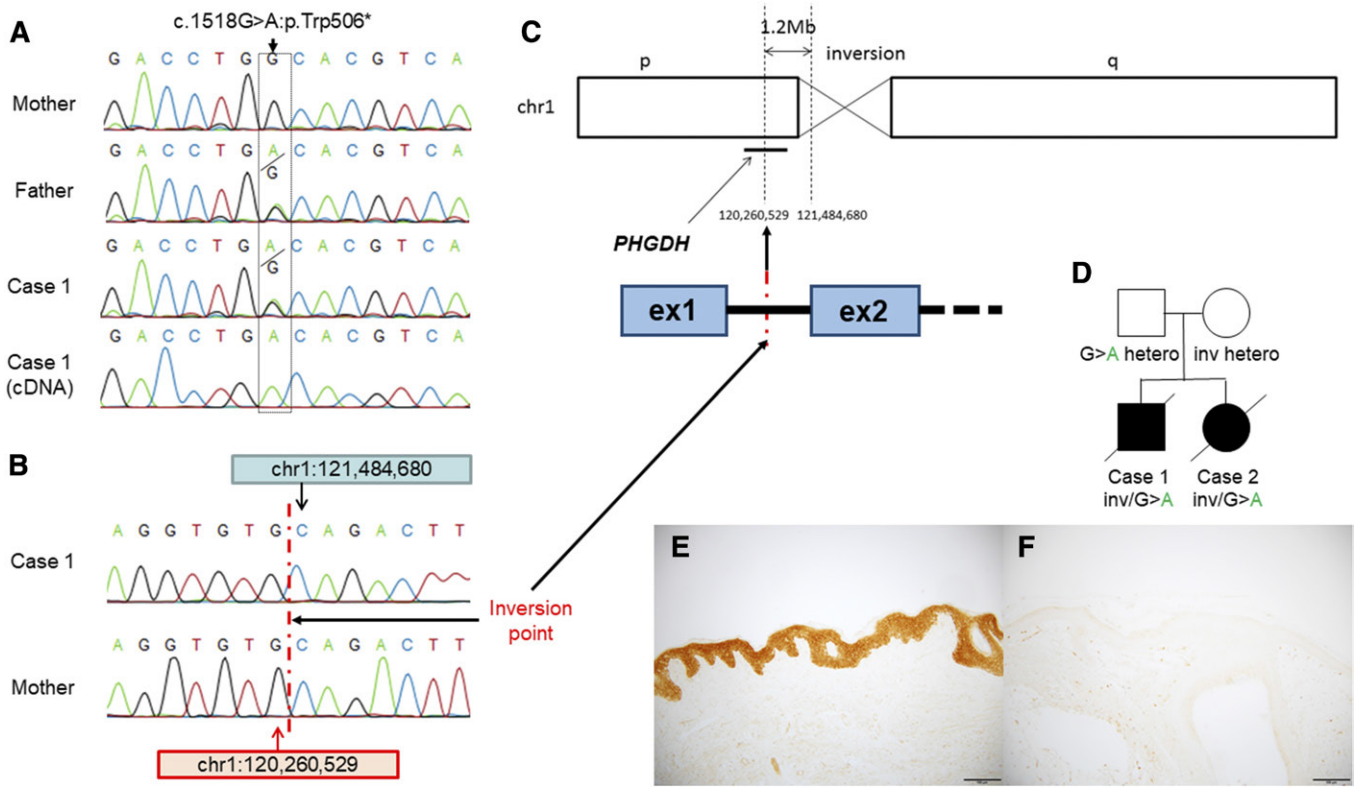

Fig. 3. Molecular characterization of the patient with Neu-Laxova syndrome (Case 1). A: Sanger sequencing confirms the heterozygous nonsense mutation c.1518G>A (p.Trp506*) in *PHGDH* in the gDNA of Case 1 and his unaffected father. The nonsense mutation is absent from the gDNA of his unaffected mother. The sequencing of cDNA using RNA extracted from the skin sample of Case 1 demonstrates a homozygous or hemizygous condition of the paternal nonsense mutation in the patient's *PHGDH* cDNA. B: Sanger sequencing shows the precise inversion point within *PHGDH* on chr 1 in Case 1 and his unaffected mother. C: Schematic of chr 1 and the location of *PHGDH*. The maternal inversion of approximately 1.2 Mb bases affects *PHGDH*. D: Pedigree of the family and segregation of the mutation. G > A means heterozygous mutations of c.1518G>A. E, F: The epidermis in a normal control skin sample (E) and in the skin sample from Case 1 (F) are stained with anti-PHDGH antibody. The amount of PHGDH is significantly reduced in the patient's epidermis compared with the normal control. Scale bars = 100 μm. inv, inversion.

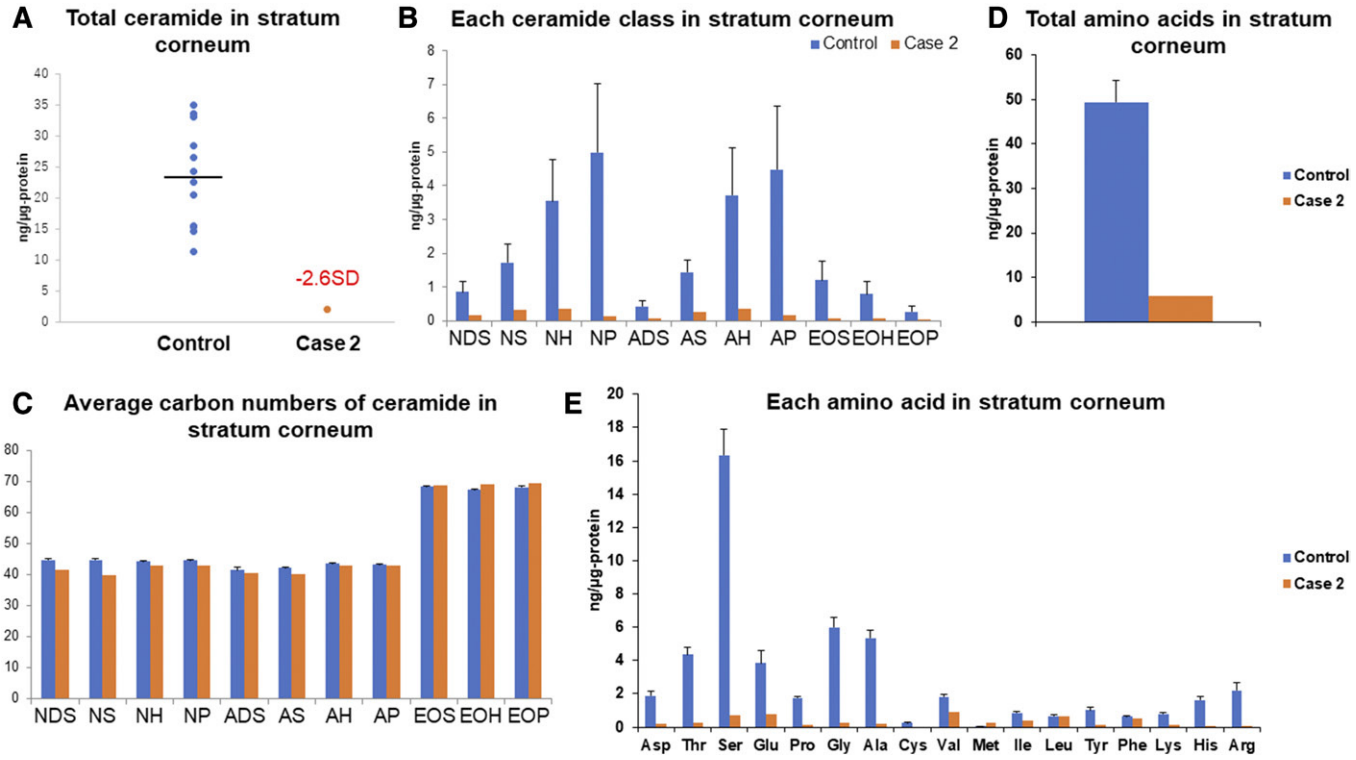

Fig. 4. Analysis of ceramides and free amino acids in the patient's stratum corneum. A, B: Amounts of total ceramide (A) and all classes of ceramide (B) in the stratum corneum of Case 2 are significantly reduced compared with those of normal controls. The total ceramide of Case 2 was 2.03 ng/μg-protein (mean − 2.6 SDs of controls). C: Average carbon numbers of 11 major ceramide species in the stratum corneum of Case 2 and normal controls. D, E: Amounts of total free amino acids (D) and each free amino acid (E) in the stratum corneum of Case 2 are significantly reduced compared with those of normal controls.

the normal controls and that CER[EOH] and CER[EOP] were increased relative to those of the normal controls (Fig. 4C), although the differences for both were not significant.

An analysis of free ultra-long-chain fatty acids (total of approximately C20–C30 linear saturated fatty acids) in the stratum corneum, as the decomposition products of sphingolipids showed a mild reduction (approximately 27%; data not shown) of the free ultra-long-chain fatty acids in Case 2 with NLS compared with those in healthy subjects.

Further, we analyzed the amount of free amino acids in the tape-stripped skin samples from Case 2 and the normal controls. The level of total amino acids was significantly lower in Case 2 than in the controls (Fig. 4D). Moreover, most of the amino acids, including L-serine, L-alanine, and L-glycine, were reduced in the Case 2 sample (Fig. 4E, supplemental Table S1).

DISCUSSION

Most of the *PHGDH* mutations that cause NLS are missense mutations, although one nonsense, one splicing, and one frameshift mutation have also been reported (3). Interestingly, biallelic null mutations have been reported in only one patient with NLS (17). Reliable genotype/phenotype correlations in *PHGDH* have not yet been clarified. Our pedigree had compound heterozygous mutations, chr 1 inversion, and p.Trp506* in *PHGDH*, and the NLS phenotypes were relatively severe (Fig. 2A, B). Severe phenotypes of NLS might be caused by truncation mutations rather than by missense mutations of *PHGDH*. We could not exclude a possible effect of another modifying factor, e.g., the heterozygous condition of chr 1 inversion, in the cases.

WES utilizes an array to capture the protein-coding regions of the human genome. These regions encompass ~20,000 genes and make up ⩽2% of the genome (18). Compared with the more than 2 to 3 million variants detected by WGS, WES typically reveals ~25,000 coding variants (19). WGS can detect mutations in noncoding regions, copy number variations, and complex chromosomal rearrangements. WES is limited in its ability to detect these variations (18). In this study, cDNA sequencing was a clue to finding the second mutation, and WGS was effective in finding it. In our pedigree, RNA analysis and genome sequencing were essential in detecting pathogenic mutations, and the combined use of powerful current techniques brought a significant benefit to the family.

The autopsy findings of Case 1 revealed liver fibrosis and hemophagocytic lymphohistiocytosis (Fig. 2E, F). Taken together with the ceramide analyses, these results suggest that, first, recurrent systemic infections (sepsis and bacteremia) based on skin barrier defects caused continuous intrahepatic cholestasis and hemophagocytic lymphohistiocytosis. Hepatocellular injuries and fibrosis

then progressed in the liver. Finally, recurrent sepsis triggered by skin infections and dehydration led to multiple organ failure, including severe respiratory failure, resulting in the fatality. Thus, the clinical findings and course of Case 1 suggests that patients with severe reductions of ceramides in the stratum corneum have recurrent systemic infections due to skin barrier defects, resulting in a poor prognosis. If we could compensate sufficiently for the skin barrier deficiency, the patients could survive, even with severe reductions of ceramides in the stratum corneum.

Ichthyosis, which has been described in 50% of individuals with NLS, is considered a consequence of serine deficiency (3). The *PHGDH* mutations we identified in our pedigree resulted in a serious loss of PHGDH function, leading to reduced ceramide synthesis with a reduction of all ceramide classes, which was evident in our LC/MS of the tape-stripped skin samples (Fig. 3). These observations suggest a reduction in sphingolipid synthesis due to serine deficiency in the stratum corneum of the patient. Conventional *Phgdh* KO mice display severe disturbance of embryonic development, such as brain malformation with overall growth retardation, and die around embryonic day 13.5 (15, 20). An analysis of membrane lipid components in embryonic tissues of conventional *Phgdh* KO mice show that L-serine deficiency resulting from *Phgdh* deletion leads to a drastic reduction of major sphingolipids (15, 20). To our knowledge, this is the first report demonstrating the reduction of ceramides in the stratum corneum of an NLS patient due to *PHGDH* mutations. Our findings suggest that the almost complete absence of ceramides in the stratum corneum in the patient indicates the possibility that the outer epidermis relies exclusively on the de novo synthesis of serine for the synthesis of stratum corneum ceramides.

It has been demonstrated that atypical 1-deoxysphingolipids (deoxySLs) are elevated in patients with hereditary sensory and autonomic neuropathy type 1 (HSAN1) due to the loss of specificity of the serine palmitoyl transferase for serine (15). Increasing amounts of alanine (and glycine) are converted by the mutant serine palmitoyltransferase to produce toxic deoxySLs, especially deoxyceramides (15, 21). Treatment with L-serine reduces the production of these toxic compounds in HSAN1 patients by the simple completion of substrates for the serine palmitoyltransferase (22). We demonstrated that not only is L-serine reduced in the stratum corneum of Case 2 compared with the normal controls but also L-alanine and L-glycine (Fig. 4E). These findings suggest that although deoxySLs were not measured directly, the aberrant synthesis pathway of toxic deoxySLs might not be activated in the stratum corneum of NLS patients. In clinical studies, the most common skin complications of HSAN1 patients are skin ulcers, not ichthyoses (21). Taken together, these facts suggest that ichthyosis in NLS may not be caused by abnormal increases in deoxySLs.

The level of total amino acids was significantly lower in Case 2 than in the controls (Fig. 4D). We hypothesize that defective keratinization, such as from parakeratosis or hyperkeratosis, caused by insufficient serine metabolism might affect the protein degradation (protein metabolism) in the stratum corneum of NLS patients and might lead to the overall decreases in amino acid levels. Otherwise, serine is involved in the synthesis of metabolites that are involved in both DNA and amino acid synthesis, such as a tetrahydrofolate (23). Therefore, deficient synthesis of these metabolites due to serine deficiency might affect the amino acid synthesis of NLS patients.

As mentioned above, sphingolipids are known to play important roles in both water retention and epidermal permeability barrier function in the mammalian stratum corneum (24). Several studies have suggested that oral sphingolipids can favorably affect stratum corneum function in animal models. Ceramides in the stratum corneum increase significantly in hairless mice fed with a medium sphingomyelin diet and statistically tend to increase in mice fed with a high sphingomyelin diet (25). Haruta-Ono et al. (26) reported that orally administered sphingomyelin is incorporated into skin sphingomyelin and converted to stratum corneum ceramides in hairless mice, a process that is involved in water retention of the stratum corneum. In addition, dietary milk phospholipids might modulate covalently bound epidermal ceramides associated with the formation of lamellar structures and suppress skin inflammation in hairless mice, resulting in improved skin barrier function (27). In hairless mice, dietary sphingomyelin modulates epidermal structures and prevents disruption of skin barrier function after UVB irradiation (28). Thus, the oral or injectional administration of sphingolipids might have been helpful in improving the skin barrier defects in the present patients.

Mutations in a number of genes have been identified in both syndromic- and nonsyndromic ichthyoses (29). Several genes/molecules among them are involved in the synthesis and metabolism of epidermal lipids (Fig. 1) (7). We recently obtained important information on ultra-long-chain acylceramide synthesis, metabolism, and transport from the newly elucidated pathogenesis of congenital ichthyoses (30). The mechanisms of the synthesis, metabolism, and dynamics of epidermal lipids, mainly ceramides, and the pathogenesis of ichthyosis have been rapidly clarified (30). We recently revealed ceramide abnormalities in the stratum corneum of many congenital ichthyoses (9, 14). The present article is the first to reveal the reduction of ceramides in the stratum corneum of an NLS patient associated with PHGDH deficiency. Ceramide deficiency, especially of EOS, is thought to be the major cause of congenital ichthyosis (30). In this study, a significant reduction of ceramides, including EOS, was shown in the stratum corneum of an NLS patient. Our results clearly demonstrate that the ichthyosis seen in NLS is an ichthyosis caused by a deficiency of stratum corneum ceramides. The ceramide reduction is considered to be a consequence of L-serine deficiency due to the loss of function of PHGDH. It is noteworthy that defective L-serine supply in NLS occurs at the most upstream position in the ceramide synthesis pathway among the genetic defects that cause ceramide deficiency-associated congenital ichthyosis and ichthyosis syndromes.

REFERENCES

1. Shaheen, R., Z. Rahbeeni, A. Alhashem, E. Faqeih, Q. Zhao, Y. Xiong, A. Almoisheer, S. M. Al-Qattan, H. A. Almadani, N. Al-Onazi, et al. 2014. Neu-Laxova syndrome, an inborn error of serine metabolism, is caused by mutations in PHGDH. *Am. J. Hum. Genet.* **94:** 898–904.
2. Acuna-Hidalgo, R., D. Schanze, A. Kariminejad, A. Nordgren, M. H. Kariminejad, P. Conner, G. Grigelioniene, D. Nilsson, M. Nordenskjöld, A. Wedell, et al. 2014. Neu-Laxova syndrome is a heterogeneous metabolic disorder caused by defects in enzymes of the L-serine biosynthesis pathway. *Am. J. Hum. Genet.* **95:** 285–293.
3. El-Hattab, A. W., R. Shaheen, J. Hertecant, H. I. Galadari, B. S. Albaqawi, A. Nabil, and F. S. Alkuraya. 2016. On the phenotypic spectrum of serine biosynthesis defects. *J. Inherit. Metab. Dis.* **39:** 373–381.
4. Jaeken, J., M. Detheux, L. Van Maldergem, M. Foulon, H. Carchon, and E. Van Schaftingen. 1996. 3-Phosphoglycerate dehydrogenase deficiency: an inborn error of serine biosynthesis. *Arch. Dis. Child.* **74:** 542–545.
5. Pind, S., E. Slominski, J. Mauthe, K. Pearlman, K. J. Swoboda, J. A. Wilkins, P. Sauder, and M. R. Natowicz. 2002. V490M, a common mutation in 3-phosphoglycerate dehydrogenase deficiency, causes enzyme deficiency by decreasing the yield of mature enzyme. *J. Biol. Chem.* **277:** 7136–7143.
6. Holleran, W. M., Y. Takagi, and Y. Uchida. 2006. Epidermal sphingolipids: metabolism, function, and roles in skin disorders. *FEBS Lett.* **580:** 5456–5466.
7. Kihara, A. 2016. Synthesis and degradation pathways, functions, and pathology of ceramides and epidermal acylceramides. *Prog. Lipid Res.* **63:** 50–69.
8. Linn, S. C., H. S. Kim, E. M. Keane, L. M. Andras, E. Wang, and A. H. Jr. Merrill. 2001. Regulation of de novo sphingolipid biosynthesis and the toxic consequences of its disruption. *Biochem. Soc. Trans.* **29:** 831–835.
9. Takeichi, T., A. Torrelo, J. Y. W. Lee, Y. Ohno, M. L. Lozano, A. Kihara, L. Liu, Y. Yasuda, J. Ishikawa, T. Murase, et al. 2017. Biallelic mutations in KDSR disrupt ceramide synthesis and result in a spectrum of keratinization disorders associated with thrombocytopenia. *J. Invest. Dermatol.* **137:** 2344–2353.
10. Li, H., and R. Durbin. 2010. Fast and accurate long-read alignment with Burrows-Wheeler transform. *Bioinformatics.* **26:** 589–595.
11. Thorvaldsdóttir, H., J. T. Robinson, and J. P. Mesirov. 2013. Integrative Genomics Viewer (IGV): high-performance genomics data visualization and exploration. *Brief. Bioinform.* **14:** 178–192.
12. Takeichi, T., N. Watanabe, Y. Muro, S. Teshigawara, M. Sato, N. Ban, and M. Akiyama. 2017. Phosphorylated signal transducer and activator of transcription 3 in the epidermis in adult-onset Still's disease. *J. Dermatol.* **44:** 1172–1175.
13. Ishikawa, J., Y. Shimotoyodome, S. Ito, Y. Miyauchi, T. Fujimura, T. Kitahara, and T. Hase. 2013. Variations in the ceramide profile in different seasons and regions of the body contribute to stratum corneum functions. *Arch. Dermatol. Res.* **305:** 151–162.
14. Ohno, Y., S. Nakamichi, A. Ohkuni, N. Kamiyama, A. Naoe, H. Tsujimura, U. Yokose, K. Sugiura, J. Ishikawa, M. Akiyama, et al. 2015. Essential role of the cytochrome P450 CYP4F22 in the production of acylceramide, the key lipid for skin permeability barrier formation. *Proc. Natl. Acad. Sci. USA.* **112:** 7707–7712.
15. Esaki, K., T. Sayano, C. Sonoda, T. Akagi, T. Suzuki, T. Ogawa, M. Okamoto, T. Yoshikawa, Y. Hirabayashi, and S. Furuya. 2015. L-serine deficiency elicits intracellular accumulation of cytotoxic deoxysphingolipids and lipid body formation. *J. Biol. Chem.* **290:** 14595–14609.
16. Fukagawa, S., S. Haramizu, S. Sasaoka, Y. Yasuda, H. Tsujimura, and T. Murase. 2017. Coffee polyphenols extracted from green coffee beans improve skin properties and microcirculatory function. *Biosci. Biotechnol. Biochem.* **81:** 1814–1822.
17. Mattos, E. P., A. A. Silva, J. A. Magalhães, J. C. Leite, S. Leistner-Segal, R. Gus-Kessler, J. A. Perez, L. M. Vedolin, A. Torreblanca-Zanca, P. Lapunzina, et al. 2015. Identification of a premature stop codon mutation in the PHGDH gene in severe Neu-Laxova syndrome-evidence for phenotypic variability. *Am. J. Med. Genet. A.* **167:** 1323–1329.
18. Salam, A., M. A. Simpson, K. L. Stone, T. Takeichi, A. Nanda, M. Akiyama, and J. A. McGrath. 2014. Next generation diagnostics of heritable connective tissue disorders. *Matrix Biol.* **33:** 35–40.
19. Singleton, A. B. 2011. Exome sequencing: a transformative technology. *Lancet Neurol.* **10:** 942–946.
20. Yoshida, K., S. Furuya, S. Osuka, J. Mitoma, Y. Shinoda, M. Watanabe, N. Azuma, H. Tanaka, T. Hashikawa, S. Itohara, et al. 2004. Targeted disruption of the mouse 3-phosphoglycerate dehydrogenase gene causes severe neurodevelopmental defects and results in embryonic lethality. *J. Biol. Chem.* **279:** 3573–3577.
21. Houlden, H., R. King, J. Blake, M. Groves, S. Love, C. Woodward, S. Hammans, J. Nicoll, G. Lennox, D. G. O'Donovan, et al. 2006. Clinical, pathological and genetic characterization of hereditary sensory and autonomic neuropathy type 1 (HSAN I). *Brain.* **129:** 411–425.
22. Garofalo, K., A. Penno, B. P. Schmidt, H. J. Lee, M. P. Frosch, A. von Eckardstein, R. H. Brown, T. Hornemann, and F. S. Eichler. 2011. Oral L-serine supplementation reduces production of neurotoxic deoxysphingolipids in mice and humans with hereditary sensory autonomic neuropathy type 1. *J. Clin. Invest.* **121:** 4735–4745.
23. El-Hattab, A. W. 2016. Serine biosynthesis and transport defects. *Mol. Genet. Metab.* **118:** 153–159.
24. Tsuji, K., S. Mitsutake, J. Ishikawa, Y. Takagi, M. Akiyama, H. Shimizu, T. Tomiyama, and Y. Igarashi. 2006. Dietary glucosylceramide improves skin barrier function in hairless mice. *J. Dermatol. Sci.* **44:** 101–107.
25. Haruta-Ono, Y., H. Ueno, N. Ueda, K. Kato, and T. Yoshioka. 2012. Investigation into the dosage of dietary sphingomyelin concentrate in relation to the improvement of epidermal function in hairless mice. *Anim. Sci. J.* **83:** 178–183.
26. Haruta-Ono, Y., S. Setoguchi, H. M. Ueno, S. Higurashi, N. Ueda, K. Kato, T. Saito, K. Matsunaga, and J. Takata. 2012. Orally administered sphingomyelin in bovine milk is incorporated into skin sphingolipids and is involved in the water-holding capacity of hairless mice. *J. Dermatol. Sci.* **68:** 56–62.
27. Morifuji, M., C. Oba, S. Ichikawa, K. Ito, K. Kawahata, Y. Asami, S. Ikegami, H. Itoh, and T. Sugawara. 2015. A novel mechanism for improvement of dry skin by dietary milk phospholipids: effect on epidermal covalently bound ceramides and skin inflammation in hairless mice. *J. Dermatol. Sci.* **78:** 224–231.
28. Oba, C., M. Morifuji, S. Ichikawa, K. Ito, K. Kawahata, T. Yamaji, Y. Asami, H. Itou, and T. Sugawara. 2015. Dietary milk sphingomyelin prevents disruption of skin barrier function in hairless mice after UV-B irradiation. *PLoS One.* **10:** e0136377.
29. Takeichi, T., and M. Akiyama. 2016. Inherited ichthyosis: nonsyndromic forms. *J. Dermatol.* **43:** 242–251.
30. Akiyama, M. 2017. Corneocyte lipid envelope (CLE), the key structure for skin barrier function and ichthyosis pathogenesis. *J. Dermatol. Sci.* **88:** 3–9.